



## The Combining Effect of Inclination Angle, Aspect Ratio and Thermal Loading on the Dynamic Response of Clamped-Clamped Pipe Conveying Fluid

Jabbar H. Mohmmmed \*, Mauwafak A. Tawfik, Qasim A. Atiyah 

Mechanical Engineering Department, University of Technology -Iraq, Alsina'a street, 10066 Baghdad, Iraq.

\*Corresponding author Email: [21955@student.uotechnology.edu.iq](mailto:21955@student.uotechnology.edu.iq)

### HIGHLIGHTS

- Temperature variation, inclination angle, and aspect ratio have strongly affected on vibration characteristics of pipe-fluid system.
- Thermal effects in the pipe are very important factor and more significant in comparison with the internal fluid velocity.
- Inclination angle has larger impact on vibration characteristics at higher aspect ratio.

### ABSTRACT

The investigation of the vibration of pipes containing flowing fluid is very essential to obtain an understanding of their dynamic behavior and prevent their catastrophic failure due to fatigue. Pipelines are subjected to environmental static and dynamic loading including self-weight, restoring, and Coriolis forces. This research aims to investigate the vibrations of pipeline structures for examining their structural integrity under these conditions. A linear Euler-Bernoulli beam model is used to analyze the dynamic response of flexible, inclined, and fixed ends pipe conveying fluid made of polypropylene random-copolymer. Closed-form expression for dynamic response is presented by using combining of finite Fourier sine and Laplace transforms method. The influences of the inclination angle, thermal load, and aspect ratio (ratio of outside diameter to the length of pipe) on the dynamical behavior of the pipe-fluid system are studied. The obtained results attest to the importance of considering combining effects of the inclination angle, thermal load, and aspect ratio in analyzing and designing pipe conveying fluid. It is observed that the dynamic deflection can be significantly increased by increasing temperature, aspect ratio, and fluid velocity, while it reduced by increasing the inclination angle with the horizontal axis in the range of (0-90).

### ARTICLE INFO

**Handling editor:** Muhsin J. Jweeg

**Keywords:**

Pipe conveying fluid  
Dynamic Response  
Thermal Effect  
Inclined Pipe  
Finite Fourier sine transform  
Laplace transform

### 1. Introduction

Modern improvements in engineering materials and cost reduction have made the investigation of the vibration characteristics of pipes containing flowing fluid to be an essential issue. This problem arises from the fact that the dynamic behavior of a component can be strongly changed when it is in contact with the fluid. Fluid force effect on structure movement at the interface region between the two domains, and consequently the new position of the structure can affect the flowing fluid. These oscillations can lead to damage to the components and instabilities may occur. Hence, for practical applications, it is necessary to be able to catch the dynamical behavior up to which the component can lose its stable behavior [1]. Pipelines containing flowing fluid play a very important role in industrial applications and they are common components in many engineering fields that can be found in aviation, cosmonautics, chemical, oil and gas automotive, and marine industries [2, 3]. Therefore, how to get the dynamic behavior of elastic pipes became a hot topic leading to a good number of studies, over the past 50 years, about the linear and nonlinear dynamics of pipes conveying fluid with different end conditions [3-10].

Recently, Ze-Qi Lu et al. [11] investigated the effect of vibration on fatigue strength of fixed end pipe conveying fluid. They found that internal resonance can reduce the fatigue life of pipes. Pipe with variable wall thickness was analyzed by Y. Amine et al. [12]. It is demonstrated that the effect of Coriolis forces is more important at a higher mass ratio  $\beta$ . D.B. Jacobi et al. [13] studied numerically and analytically the effect of varying density on the dynamic behavior of pipes conveying fluid. Their most important finding was that the density affects stability most crucially at the discharging end of the pipe. The

influences of adding point masses and springs on the stability of horizontal and vertical pipelines containing flowing fluid were studied by J. El Najjar, and F. Daneshmand [14]. They observed the possibility of increasing the critical flow velocity by adding a spring and a point mass at specific positions depending on the mass ratio  $\beta$  of the system. An overview that summarizes the mechanical behavior of pipes containing flowing fluid was presented by R. A. Ibrahim [15]. He discusses pipe-fluid system problems including various types of modeling, dynamic analysis, and stability regimes of pipes containing flowing fluid under different types of end conditions, working environments, and geometrical parameters. Most of the previous studies adopt numerical or approximate approaches, like the Galleria method [14], transfer matrix [16], finite element [17], etc., hence, an attempt was performed in the current study to present an analytical solution for pipe conveying fluid problem based on integral transform technique by using a mixing of finite Fourier sine and Laplace transforms. For the time being, thermal fluid-structure analysis plays a major role in modern technologies. Frequently, the separate consideration of the structural mechanics, fluid mechanics, and heat transfer does not reflect the real case because there are significant coupling influences such as a deformed structure as a result of thermal expansion and fluid loads or heat transfer due to the friction of a fluid. Thus, one of the objectives of the current study is to consider the effect of thermal loading on the dynamic response of pipes that flow inside its incompressible fluid. On the other hand, from observing available studies, it is clear that the dynamic behavior of pipelines containing flowing fluid has been investigated quite extensively and important results have been accomplished. However, few studies treat inclined systems and the influences of the inclination angle on the dynamic characteristics of the systems. The dynamic response of the inclined pipe is somewhat different from that of the horizontal or vertical pipe because of an additional deflection of the inclined pipe due to the gravitational component. It should also be noted that most of the scholars have not studied the related issues that operate under the thermal environment, which makes the current study on this subject necessary. To compensate for the lack of ongoing research as mentioned above, the present work is aimed at studying the combining effects of the supported angle, aspect ratio, and temperature variation on the dynamical behavior of a clamped-clamped pipe conveying fluid, which, to our knowledge, has never been previously examined. A closed analytical form solution for the equation of motion was offered by using the mixing of finite Fourier sine and Laplace transforms.

## 2. Equation of motion

The system under consideration is illustrated in Figure 1 that comprises an elastic inclined pipe of length  $L$ , flexural rigidity  $EI$ , cross-section  $A_p$  with mass per unit length  $m_p$ . The pipe is fixed at both ends and contains an incompressible flowing fluid with mass per unit length  $m_f$  and mean axial flow velocity  $U$  which is assumed to be uniform across the pipe cross-section.

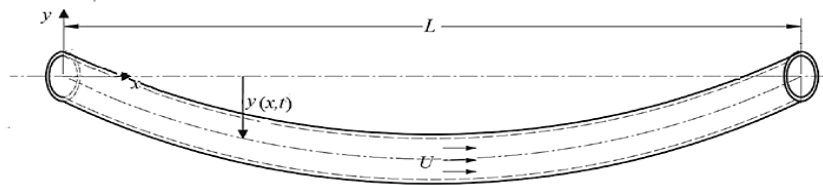


Figure 1: Schematic of the pipe conveying fluid

By ignoring internal damping, dissipation, external tension, and internal pressurization, the equation of motion for the inclined pipe conveying fluid under thermal loading is obtained as [18, 19]:

$$EI \frac{\partial^4 y}{\partial x^4} - [(m_f + m_p)(L - x)g \sin \theta - N - m_f U^2] \frac{\partial^2 y}{\partial x^2} + (m_f + m_p)g \sin \theta \frac{\partial y}{\partial x} + (m_f + m_p)g \cos \theta + 2m_f U \frac{\partial^2 y}{\partial x \partial t} + (m_f + m_p) \frac{\partial^2 y}{\partial t^2} = 0 \quad (1)$$

Where  $g$  is the acceleration of gravity,  $\theta$  is the support angle between the pipe and the horizontal axis,  $N$  is thermal load,  $y(x, t)$  is the lateral displacement of the pipe;  $x$  and  $t$  are the axial coordinate and time, respectively.  $N$  can be determined by the formula:

$$N = \alpha A_p E \Delta T \quad (2)$$

Where  $\alpha$  is the coefficient of thermal expansion ( $1/^\circ\text{C}$ ),  $L$  is the pipe length (m).  $\Delta T = T_x - T_i$  is the temperature difference ( $^\circ\text{C}$ ).  $T_i$  is the laboratory temperature ( $^\circ\text{C}$ ),  $T_x$  is the instantaneous temperature ( $^\circ\text{C}$ ).

Equation 1 always can be rewritten in dimensionless form as

$$\frac{\partial^4 \phi}{\partial \zeta^4} - [(1 - \zeta)G \sin \theta - \bar{N} - v^2] \frac{\partial^2 \phi}{\partial \zeta^2} + G \sin \theta \frac{\partial \eta}{\partial \zeta} + G \cos \theta + \frac{\partial^2 \phi}{\partial \tau^2} - 2\beta^{\frac{1}{2}} v \frac{\partial^2 \phi}{\partial \zeta \partial \tau} = 0 \quad (3)$$

Where;

$$\phi = \frac{y}{L}, \quad \zeta = \frac{x}{L}, \quad \beta = \frac{m_f}{m_f + m_p}, \quad G = \frac{(m_f + m_p)gL^3}{EI}, \quad v = \left(\frac{m_f}{EI}\right)^{\frac{1}{2}} UL, \quad \bar{t} = \frac{1}{L^2} \left(\frac{EI}{m_f + m_p}\right)^{\frac{1}{2}}$$

In other forms

$$\phi'''' - [(1 - \zeta)G \sin \theta - \bar{N} - v^2]\phi'' + G \sin \theta \phi' + 2\beta^{\frac{1}{2}} v \phi' + \ddot{\phi} = -G \cos \theta \tag{4}$$

### 2.1 Solution method

Equation 3 can be discreted and transformed into an ordinary differential equation by introducing the term  $\phi(\zeta, \tau)$  to decompose the equation into space and time as follows

$$\phi(\zeta, \bar{t}) = \Gamma(\zeta)\Lambda(\bar{t}) \tag{5}$$

Where  $\Lambda(\bar{t})$  the generalized coordinate of the system and  $\Gamma(\zeta)$  are trial/comparison functions satisfying both the geometrical and natural boundary conditions by substituting (5) in (4)

$$\Gamma''''(\zeta)\Lambda(\bar{t}) - [(1 - \zeta)G \sin \theta - \bar{N} - v^2]\Gamma''(\zeta)\Lambda(\bar{t}) + G \sin \theta \Gamma'(\zeta)\Lambda(\bar{t}) + G \cos \theta + 2\beta^{\frac{1}{2}} v \Gamma'(\zeta)\Lambda(\bar{t}) + \Gamma(\zeta)\ddot{\Lambda}(\bar{t}) = 0 \tag{6}$$

To suppress the time dependency, the Laplace transform was introduced by assuming zero initial conditions case.

$$\Gamma''''(\zeta)\Lambda(s) - [(1 - \zeta)G \sin \theta - \bar{N} - v^2]\Gamma''(\zeta)\Lambda(s) + G \sin \theta \Gamma'(\zeta)\Lambda(s) + \frac{G}{s} \cos \theta + 2\beta^{\frac{1}{2}} v \Gamma'(\zeta)s\Lambda(s) + \Gamma(\zeta)s^2\Lambda(s) = 0 \tag{7}$$

Then, a finite Fourier sine transform was introduced to convert eq. 6 into superimposed double degrees of freedom system.

$$\Lambda(s) \int_0^1 \Gamma''''(\zeta) \sin n\pi\zeta d\zeta - [G \sin \theta - \bar{N} - v^2]\Lambda(s) \int_0^1 \Gamma''(\zeta) \sin n\pi\zeta d\zeta + G \sin \theta \Lambda(s) \int_0^1 \zeta \Gamma''(\zeta) \sin n\pi\zeta d\zeta + G \sin \theta \Lambda(s) \int_0^1 \Gamma'(\zeta) \sin n\pi\zeta d\zeta + 2\beta^{\frac{1}{2}} v s \Lambda(s) \int_0^1 \Gamma'(\zeta) \sin n\pi\zeta d\zeta + s^2 \Lambda(s) \int_0^1 \Gamma(\zeta) \sin n\pi\zeta d\zeta = -\frac{G}{s} \cos \theta \int_0^1 (1) \sin n\pi\zeta d\zeta \tag{8}$$

$\Gamma(\zeta)$  Is beam Eigen functions, for clamped support case and in polynomial form we have:

$$\Gamma(\zeta) = a_0 + a_1\zeta + a_2\zeta^2 + a_3\zeta^3 + a_4\zeta^4 \tag{9}$$

Applying the boundary conditions for clamped support

$$\text{at } \zeta = 0, \quad \phi = 0 \text{ and } \partial\phi/\partial\zeta = 0, \quad \text{at } \zeta = 1, \quad \phi = 0 \text{ and } \partial\phi/\partial\zeta = 0$$

Gives

$$\Gamma(\zeta) = (\zeta^4 - 2\zeta^3 + \zeta^2)a_4 \tag{10}$$

By using orthogonal functions, it can be obtained

$$a_4 = 3\sqrt{70} \left( \frac{1}{\sqrt{a^5(70a^4 - 315a^3 + 540a^2 - 420a + 126)}} \right) \tag{11}$$

For  $a = 1$ , it can be find  $a_4 = 25.20$  for the first mode. Furthermore, noting that

$$\left. \begin{aligned} \int_0^1 Y(\xi) \sin n\pi\xi d\xi &= \frac{24}{n^5\pi^5} (1 + (-1)^{n+1}) - \frac{2}{n^3\pi^3} (1 + (-1)^{n+1}) \\ \int_0^1 Y'(\xi) \sin n\pi\xi d\xi &= \frac{12}{n^3\pi^3} (1 + (-1)^n) \\ \int_0^1 Y''(\xi) \sin n\pi\xi d\xi &= \frac{2}{n\pi} (1 + (-1)^{n+1}) - \frac{24}{n^3\pi^3} (1 + (-1)^{n+1}) \\ \int_0^1 \xi Y''(\xi) \sin n\pi\xi d\xi &= \frac{24}{n^3\pi^3} (1 + 2(-1)^n) + \frac{2(-1)^{n+1}}{n\pi} \\ \int_0^1 Y''''(\xi) \sin n\pi\xi d\xi &= \frac{24}{n\pi} (1 + (-1)^{n+1}) \\ \int_0^1 (1) \sin n\pi\xi d\xi &= \frac{(1+(-1)^{n+1})}{n\pi} = 1^F \end{aligned} \right\} \quad (12)$$

On substituting eq. (12) in eq. (8)

$$\begin{aligned} &\frac{24}{n\pi} (1 + (-1)^{n+1})q(s) - [\bar{g} \sin \theta - \bar{N} - v^2] \left( \frac{2}{n\pi} (1 + (-1)^{n+1}) - \frac{24}{n^3\pi^3} (1 + (-1)^{n+1}) \right) q(s) + \\ &\bar{g} \sin \theta \left( \frac{24}{n^3\pi^3} (1 + 2(-1)^n) + \frac{2(-1)^{n+1}}{n\pi} \right) q(s) + \bar{g} \sin \theta \frac{12}{n^3\pi^3} (1 + (-1)^n) q(s) - 2\beta^{\frac{1}{2}} v s \frac{12}{n^3\pi^3} (1 + \\ &(-1)^n) q(s) + s^2 \left( \frac{24}{n^5\pi^5} (1 + (-1)^{n+1}) - \frac{2}{n^3\pi^3} (1 + (-1)^{n+1}) \right) q(s) = -\frac{\bar{g}}{s} \cos \theta \ 1(\mathcal{F}) \end{aligned} \quad (13)$$

Rearrange

$$\begin{aligned} &\left[ s^2 \left( \frac{24}{n^5\pi^5} (1 + (-1)^{n+1}) - \frac{2}{n^3\pi^3} (1 + (-1)^{n+1}) \right) + s \left( 2\beta^{\frac{1}{2}} v \left( \frac{12}{n^3\pi^3} (1 + (-1)^n) \right) \right) + \right. \\ &\frac{24}{n\pi} (1 + (-1)^{n+1}) - [\bar{N} + v^2] \left( \frac{2}{n\pi} (1 + (-1)^{n+1}) - \frac{24}{n^3\pi^3} (1 + (-1)^{n+1}) \right) + \\ &G \sin \theta \left( \frac{2}{n\pi} (1 + (-1)^{n+1}) - \frac{24}{n^3\pi^3} (1 + (-1)^{n+1}) + \frac{24}{n^3\pi^3} (1 + 2(-1)^n) + \frac{2(-1)^{n+1}}{n\pi} + \right. \\ &\left. \left. \frac{12}{n^3\pi^3} (1 + (-1)^n) \right) \right] \Lambda(s) = -\frac{G}{s} \cos \theta \ 1(\mathcal{F}) \end{aligned} \quad (14)$$

Let

$$Z_{f1} = 2\beta^{\frac{1}{2}} v \left( \frac{12}{n^3\pi^3} (1 + (-1)^n) \right) \quad (15)$$

$$\begin{aligned} Z_{f2} &= \frac{24}{n\pi} (1 + (-1)^{n+1}) - [\bar{N} + v^2] \left( \frac{2}{n\pi} (1 + (-1)^{n+1}) - \frac{24}{n^3\pi^3} (1 + (-1)^{n+1}) \right) + \\ G \sin \theta &\left( \frac{2}{n\pi} (1 + (-1)^{n+1}) - \frac{24}{n^3\pi^3} (1 + (-1)^{n+1}) + \frac{24}{n^3\pi^3} (1 + 2(-1)^n) + \frac{2(-1)^{n+1}}{n\pi} + \frac{12}{n^3\pi^3} (1 + \right. \\ &(-1)^n) \end{aligned} \quad (16)$$

$$\therefore \left[ s^2 \frac{24}{n^5\pi^5} (1 + (-1)^{n+1}) + Z_{f1}s + Z_{f2} \right] \Lambda(s) = -\frac{G}{s} \cos \theta \ 1(\mathcal{F}) \quad (17)$$

Moreover, it can assume,

$$\phi_{f1} = \frac{Z_{f1}}{\frac{24}{n^5\pi^5}(1+(-1)^{n+1}) - \frac{2}{n^3\pi^3}(1+(-1)^{n+1})} \quad (18)$$

$$\phi_f^2 = \frac{Z_{f2}}{\frac{24}{n^5\pi^5}(1+(-1)^{n+1}) - \frac{2}{n^3\pi^3}(1+(-1)^{n+1})} \quad (19)$$

$$\therefore \Lambda(s) = \frac{-\frac{G}{s} \cos \theta \ 1(\mathcal{F})}{\frac{24}{n^5\pi^5}(1+(-1)^{n+1}) - \frac{2}{n^3\pi^3}(1+(-1)^{n+1})} \left[ s^2 + \phi_{f1}s + \phi_f^2 \right] \quad (20)$$

By applying the Fourier-Laplace inversion, the dynamic response for inclined, fixed supported pipe conveying fluid can be obtained:

$$\phi(\zeta, \bar{t}) = \Gamma(\zeta) \frac{-G \cos \theta F_f(\bar{t})}{\frac{24}{n^4 \pi^4} \frac{2}{n^2 \pi^2}} \tag{21}$$

$$F_f(\bar{t}) = \left( \frac{1}{\alpha_{f1} \alpha_{f2}} + \frac{1}{\alpha_{f1} \alpha_{f2} (\alpha_{f2} - \alpha_{f1})} (\alpha_{f1} e^{-\alpha_{f2} \bar{t}} - \alpha_{f2} e^{-\alpha_{f1} \bar{t}}) \right) \tag{22}$$

$$\alpha_{f1} = \frac{\phi_{f1}}{2} + i \sqrt{\phi_f^2 - \frac{\phi_{f1}^2}{4}}, \alpha_{f2} = \frac{\phi_{f1}}{2} - i \sqrt{\phi_f^2 - \frac{\phi_{f1}^2}{4}} \tag{23}$$

### 3. Results and discussion

In this section, the results of the analytic solution of the equation of motion of the pipe-fluid system were described. The main characteristics of the pipe and fluid and the numeric parameters considered in the current work are shown in Table 1 and all results were simulated in MATLAB 2019b software.

**Table 1:** Numeric values of used parameter

Specification	Unit	Value
Material	—	PPR
Fluid	—	Water
Outer diameter $D_o$	m	0.025
Thickness $t$	m	0.0035
Aspect ratio (length to outer diameter) $L/D_o$	—	(20 - 50) $D_o$
		0.8 at 25°C
Modulus of elasticity $E$	GPa	0.38 at 50°C
		0.23 at 70°C
Density of pipe $\rho_p$	Kg/m <sup>3</sup>	909
Density of fluid $\rho_r$	Kg/m <sup>3</sup>	1000
Coefficient of expansion $\alpha$	1/K	0.3x10 <sup>-4</sup>

For a good understanding of the overall vibration characteristics of a fixed supported pipe conveying fluid, some geometrical and systematic parameters in respect to dynamic deflection were studied. For this purpose, the lateral deflection of the fixed supported pipe conveying fluid within the entire span scope was plotted under different aspect ratios with setting  $\nu = 1, t = 0.2, T = 25, \theta = 0, n = 1$  as illustrated in Figure 2. Along with the span of the pipe, the amplitude of lateral displacement of the fixed supported pipe conveying fluid changed constantly; the lateral dynamic displacement showed asymmetric distribution relative to the mid-span position and had only one extreme value at the mid-span. With increasing the aspect ratio, the amplitude of lateral displacement becomes larger. This may be attributed to weak pipe stiffness at a higher aspect ratio due to an increase in pipe weight. The same behavior was observed in Ref. [20] with a simply supported pipe. However, the dynamic deflection for the fixed supported pipe was significantly smaller as compared with that of the simply supported pipe. This is because the lateral deflection of the pipe develops with the increase of the total number of degrees of freedom at the ends.

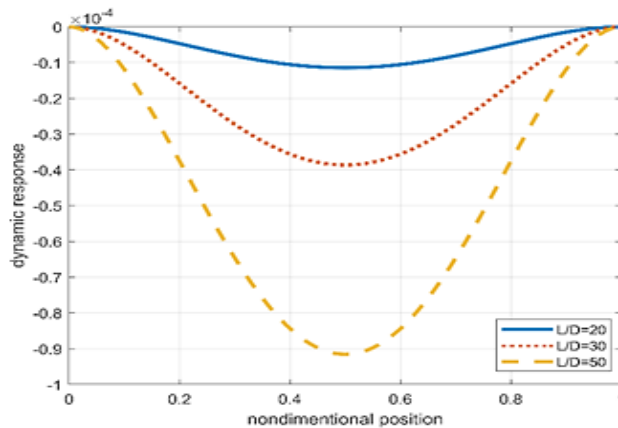


**Figure 2:** the dynamic response variation vs. span of the pipe for various aspect ratios

The effect of aspect ratio on dynamic response was further investigated by plotting the dynamic deflection against the aspect ratio at different fluid velocities, as shown in Figure 3. It can be observed that the increase of the fluid velocity value strongly affected the amplitude of dynamic deflection as the aspect ratio increased. With smaller values of the fluid velocity, dynamic deflection grew gradually to maximum values with increasing aspect ratio while further increase in fluid velocity leads to a more dramatic increase in the amplitude of dynamic deflection. This suggests that the pipe for the same fluid velocity will fail quicker with a higher aspect ratio. For further examination; the dynamic deflection response for the fixed supported pipe was plotted against the non-dimensional position under a different fluid velocity as shown in Figure 4. It can be seen from the figure, that the dynamic deflection increases and then decreases and return increases with increasing fluid velocity, i.e. the pipe fluctuates between the max peak deflection at mid-span of the pipe length and the un-deformed case, and this behavior was cyclically repeated. With each cycle, it was found that the amplitude of deflection increased with keep increasing in the fluid velocity and approaching their critical value. R. S. Reddy et al. [21] found similar observations in their research with simple support functionally graded pipe conveying pulsatile fluid. This indicates that when the fluid velocity converges the critical value the amplitude of dynamic response will undergo abrupt increasing which lead to static divergence instability. This confirms that the effective stiffness of the pipe is lost as the fluid velocity increases.

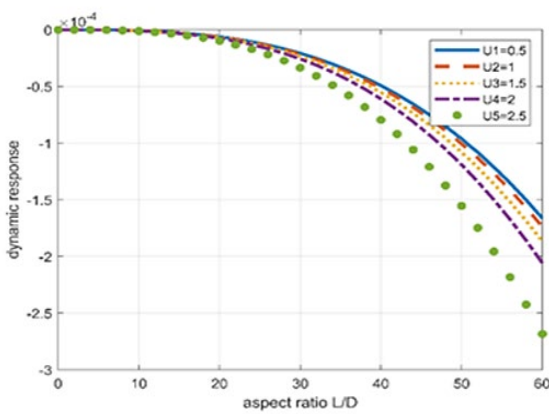


Figure 3: The dynamic response variation vs. aspect ratio for various fluid velocities

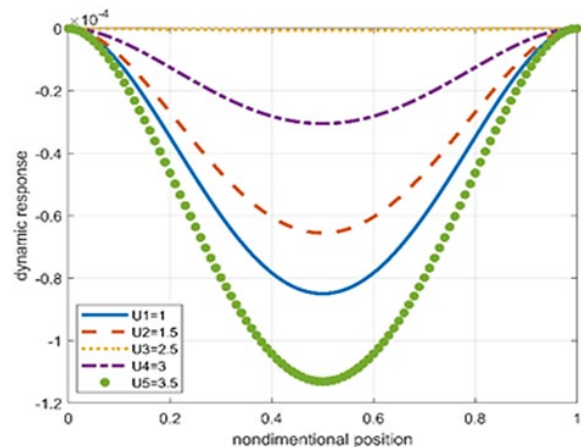


Figure 4: The dynamic response variation vs. non-dimensional position for various fluid velocities

The effect of the pipe’s inclination angle on the dynamic deflection response is studied by plotting in Figure 5 the dynamic deflection with non-dimension position normalized by various inclination angles. It can be noted from Fig. 5 that for the angles between  $0^\circ$  to  $< 90^\circ$ , as the inclination angle is increased the dynamic deflection of the pipe significantly decreases for constant temperature, aspect ratio, and fluid velocity. The maximum deflection decreases by 51.7% if the beam has an angle  $\theta = 60^\circ$  when compared to its horizontal beam ( $\theta = 0^\circ$ ) counterpart. This is associated with the lowering in the magnitude of the lateral weight component with increasing the pipe’s inclination angle, where the maximum deflection is proportional to the lateral weight component. On the other hand, at an inclination angle between  $> 90^\circ$  to  $180^\circ$  the inclined pipe starts to exhibit characteristic behavior inverse to those of an inclined pipe with angles  $< 90^\circ$  where the dynamic deflection increases as the inclination angle are increased due to the increased lateral load component with rising pipe inclination above  $\theta = 90^\circ$ . The same trend was observed by Refs. [22-24] with inclined beam subjected to a moving load.

We further examine the effect of inclination angle by plotting in Figure 6 variation of the peak mid-span of dynamic deflection of the pipe with the inclination angles  $\theta$  for different temperatures. We observe from Figure 6 that an increase in the inclination angle results in a decrease in the mid-span dynamic deflection of the fixed supported pipe and turn slightly reducing the harmful effect of increasing the temperature on the dynamic deflection of the fixed supported pipe. This decrease in dynamic deflection is very apparent in larger inclination angle more than at the lower inclination angle which can lead to enhancing the pipe-fluid system stability against the environment involving higher temperature variation. Figure 7 shows the relationship between the peak deflection of mid-span of the pipe and aspect ratio under three temperatures of the pipe, 25 (room temperature), 50, and 75, for the fixed supported pipe-fluid system. As shown in Figure 7, the peak deflection of the mid-span clearly showed dramatic increases at the highest aspect ratio with increasing pipe temperature. These suggest that there is a strong coupling between the temperature variation and aspect ratio of the pipe-fluid system. The reason is that the differences in the stiffness of the pipe are large with increasing the temperature and aspect ratio, the flexural rigidity of the pipe at temperature and aspect ratio of  $75^\circ\text{C}$  and 50 respectively is much smaller than that of the pipe at room temperature and aspect ratio of 20. Additionally, the bending resistance of the pipe at room temperature and lower aspect ratio plays a leading role in the bending resistance of the entire system.

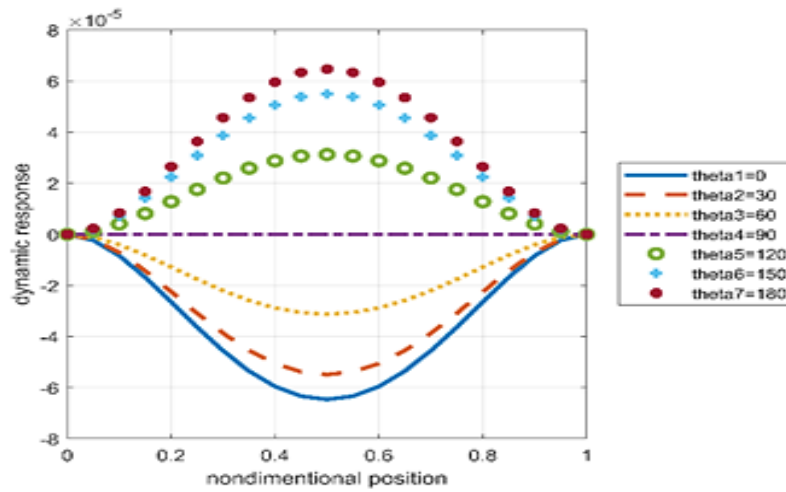


Figure 5: the dynamic response variation vs. non-dimensional position for various inclination angles

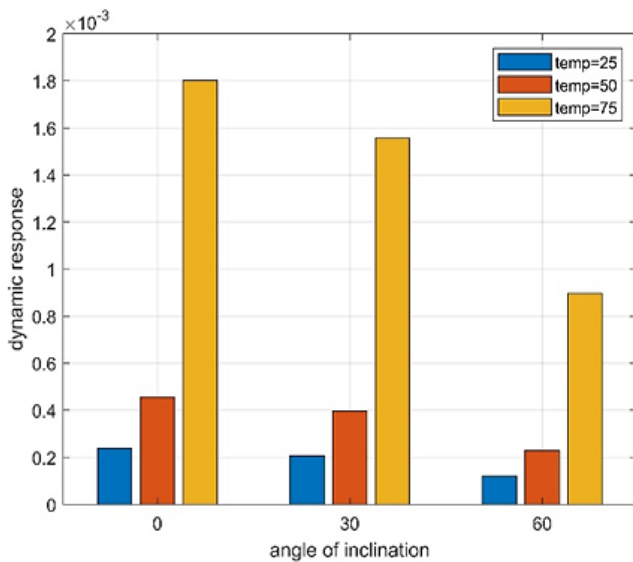


Figure 6: variation of the peak mid-span of dynamic deflection of the pipe with the inclination angles  $\theta$  for different temperatures

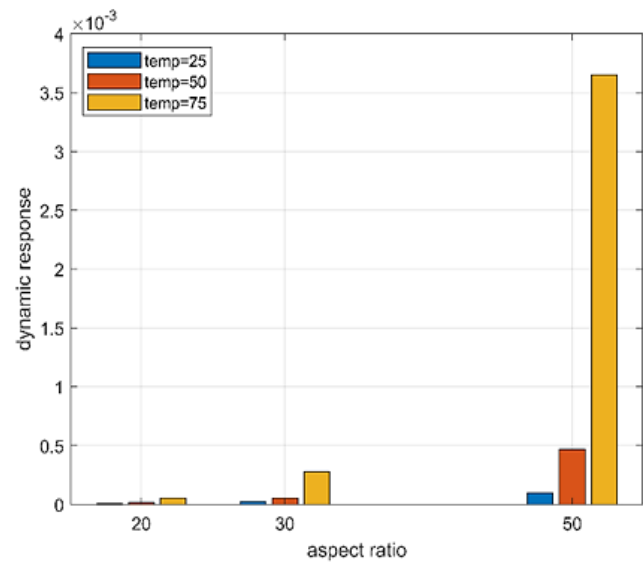
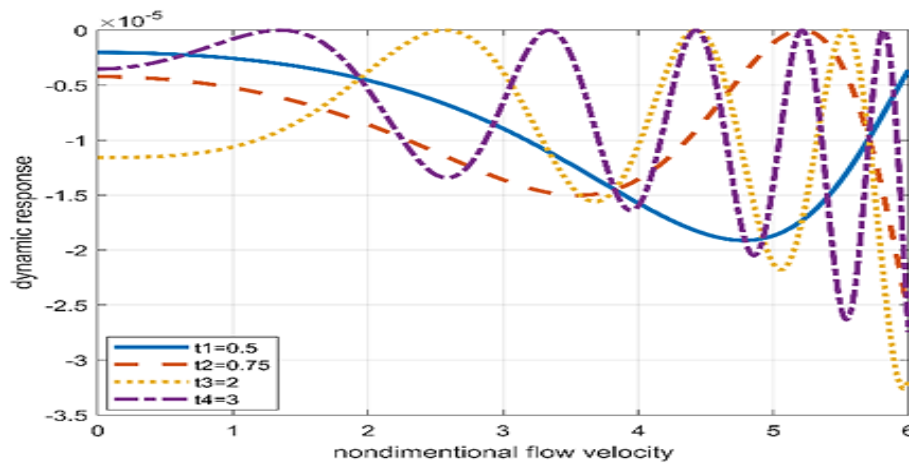


Figure 7: The maximum lateral displacement of the middle point of clamped-clamped pipe conveying fluid versus aspect ratios at different temperatures

Figure 8 illustrates the maximum lateral displacement of the middle point of clamped-clamped pipe conveying fluid versus fluid velocity at different times. With the increase in time, the influence of fluid velocity on the dynamic deflection for fixed supported pipe conveying fluid illustrates a nonlinear relationship (sine curve). The maximum lateral displacement of the middle point of the clamped-clamped pipe exhibits the variation of the sine curve. Besides, the amplitude of the sine curve increased while its period decreased with the increase of time. The results reveal that the oscillation of the pipe's middle point maximum lateral displacement increased significantly when the time and fluid velocity are increased. Moreover, the results showed that the middle point lateral displacement for the fixed supported pipe reaches the extreme value with the converging of critical velocity.



**Figure 8:** The maximum lateral displacement of the middle point of clamped-clamped pipe conveying fluid versus fluid velocity at different times

#### 4. Conclusion

It can summarize our finding from the current study as follow:

- 1) The analytical method proposed in the current study has a clear concept, suitable for hand computation, and gives a theoretical basis for more engineering applications of inclined, fixed supported pipe conveying fluid under thermal loads.
- 2) The aspect ratio temperature variation and inclination angle strongly affected both the dynamic responses of the system.
- 3) There is a strong coupling between the aspect ratio of pipe length to its outside diameter with temperature variation and inclination angle.
- 4) The temperature variation is a major concern rather than the internal fluid velocity in the design of pipe containing flowing fluid at a higher aspect ratio.
- 5) Inclination angle has a larger impact on vibration characteristics at a higher aspect ratio, which should be paid attention to in engineering.
- 6) Dynamic deflection increase with increasing temperature. The divergence can be occurring even the fluid velocity equals zero with the increasing temperature of the pipe.
- 7) Dynamic deflection increase with increasing the aspect ratio.
- 8) By increasing the pipe's inclination angle, the dynamic lateral displacement of the mid-point of the pipe decreases, and for example, at  $\theta=90^\circ$ , it becomes zero.

#### Acknowledgment

The authors gratefully acknowledge the support by the Mechanical Engineering Department at the University of Technology (UOT), Baghdad-Iraq.

#### Author contribution

All authors contributed equally to this work.

#### Funding

This research received no specific grant from any funding agency in the public, commercial, or not-for-profit sectors.

#### Data availability statement

The data that support the findings of this study are available on request from the corresponding author.

#### Conflicts of interest

The authors declare that there is no conflict of interest.

#### References

- [1] M. Paidoussis, Fluid-Structure Interactions: Slender Structures and Axial Flow, phys. sci. eng., 2 (2004).



- [2] A. R. Askarian, M. R. Permoon, M. Shakouri, Vibration analysis of pipes conveying fluid resting on a fractional Kelvin-Voigt viscoelastic foundation with general boundary conditions, *Int. J. Mech. Sci.*, 179 (2020) 105702. <https://doi.org/10.1016/j.ijmecsci.2020.105702>
- [3] R. Khodabakhsh, A. R. Saidi, R. Bahaadini, An analytical solution for nonlinear vibration and post-buckling of functionally graded pipes conveying fluid considering the rotary inertia and shear deformation effects, *Appl. Ocean. Res.*, 101 (2020) 102277. <https://doi.org/10.1016/j.apor.2020.102277>
- [4] G. W. Housner, Bending vibration of a pipe line containing flowing fluid, *J. Appl. Mech. Jun.*, 19 (1952) 205-208. <https://doi.org/10.1115/1.4010447>
- [5] R. A. Stein, M. W. Tobriner, Vibration of Pipes Containing Flowing Fluids, *J. Appl. Mech. Dec.*, 37(1970) 906-916. <https://doi.org/10.1115/1.3408717>
- [6] D. S. Weaver, T. E. Unny, On the Dynamic Stability of Fluid-Conveying Pipes, *J. Appl. Mech. Mar.*, 40 (1973) 48-52. <https://doi.org/10.1115/1.3422971>
- [7] R. H. Plaut, K. Huseyin, Instability of Fluid-Conveying Pipes under Axial Load, *J. Appl. Mech. De.*, 42 (1975) 889-890. <https://doi.org/10.1115/1.3423730>
- [8] F. J. Hatfield, D. C. Wiggert, R. S. Otwell, Fluid Structure Interaction in Piping by Component Synthesis, *J. Fluids Eng. Sep.*, 104 (1982) 318-325. <https://doi.org/10.1115/1.3241840>
- [9] M. W. Lesmez, D. C. Wigge, F. J. Hatfield, Modal Analysis of Vibrations in Liquid-Filled Piping Systems, *J. Fluids. Eng. .*, 112 (1990) 311-318. <https://doi.org/10.1115/1.2909406>
- [10] M. J. Jweeg, Z. I. Mohammad, Vibration Characteristics of Different Cross-Section Pipes with Different End Conditions, *Eng. Technol. J.*, 28 (2010) 1634-1654.
- [11] Z. Lu, K. Zhang, H. Ding, L. Chen, Nonlinear vibration effects on the fatigue life of fluid-conveying pipes composed of axially functionally graded materials, *Nonlinear. Dyn.*, 100 (2020) 1091–1104. <https://doi.org/10.1007/s11071-020-05577-8>
- [12] Y. Amini, M. Heshmati, F. Daneshmand, Dynamic behavior of conveying-fluid pipes with variable wall thickness through circumferential and axial directions, *Mar. struct.*, 72 (2020) 102758. <https://doi.org/10.1016/j.marstruc.2020.102758>
- [13] D.B. Giacobbi, C. Semler, M. P. Paidoussis, Dynamics of pipes conveying fluid of axially varying density, *J. Sound. Vib.*, 473 (2020) 115202. <https://doi.org/10.1016/j.jsv.2020.115202>
- [14] J. ElNajjar, F. Daneshmand, Stability of horizontal and vertical pipes conveying fluid under the effects of additional point masses and springs, *Ocean. Eng.*, 206 (2020) 106943. <https://doi.org/10.1016/j.oceaneng.2020.106943>
- [15] R. A. Ibrahim, Overview of Mechanics of Pipes Conveying Fluids—Part I: Fundamental Studies, *J. Pressure Vessel Technol. Jun.*, 132 (2010) 034001. <https://doi.org/10.1115/1.4001271>
- [16] Y. Dianlong, M. P. Paidoussis, H. Shen, L. Wang, Dynamic Stability of Periodic Pipes Conveying Fluid, *J. Appl. Mech. Jan.*, 81 (2014) 011008. <https://doi.org/10.1115/1.4024409>
- [17] N. Haidar, S. Obaid, M. Jawad, Instability of Angled Pipeline Arising from Internal Fluids Flow, *Iraqi J. Mech. Mater. Eng.*, 12 (2012) 223-237.
- [18] J. H. Mohammed, M. A. Tawfik, Q. A. Atiyah, Natural Frequency and Critical Velocities of Heated Inclined Pinned PP-R Pipe Conveying Fluid, *J. Achiev. Mater. Manuf. Eng.*, 107 (2021) 15-27. <https://doi.org/10.5604/01.3001.0015.2453>
- [19] M. P. Paidoussis, G. Li, Pipes Conveying Fluid: A Model Dynamical Problem, *J. Fluids Struct. .*, 7 (1993) 137-204. <https://doi.org/10.1006/jfls.1993.1011>
- [20] Q. Ni, Z. L. Zhang, L. Wang, Application of the differential transformation method to vibration analysis of pipes conveying fluid, *Appl. Math. Comput.*, 217 (2011) 7028-7038. <https://doi.org/10.1016/j.amc.2011.01.116>
- [21] R. S. Reddy, S. Panda, A. Gupta, Nonlinear dynamics of an inclined FG pipe conveying pulsatile hot fluid, *Int. J. Non-Linear Mech.*, 118 (2020) 103276. <https://doi.org/10.1016/j.ijnonlinmec.2019.103276>
- [22] J. Wu, Dynamic analysis of an inclined beam due to moving loads, *J. Sound Vib.*, 288 (2005) 107–131. <https://doi.org/10.1016/j.jsv.2004.12.020>
- [23] A. Mamandi, M. H. Kargarnovin, Dynamic analysis of an inclined Timoshenko beam traveled by successive moving masses/forces with inclusion of geometric nonlinearities, *Acta Mech.*, 218 (2011) 9–29. <https://doi.org/10.1007/s00707-010-0400-z>
- [24] A. Mamandi, M. H. Kargarnovin, D. Younesian, Nonlinear dynamics of an inclined beam subjected to a moving load, *Nonlinear Dyn.*, 60 (2010) 277–293. <https://doi.org/10.1007/s11071-009-9595-8>